Similarity between the Primary and Secondary Air-Assisted Liquid Jet Breakup Mechanisms

Yujie Wang, Kyoung-Su Im, and Kamel Fezzaa
X-Ray Science Division, Argonne National Laboratory, Argonne, Illinois 60439, USA
(Received 29 August 2007; published 18 April 2008)

We report an ultrafast synchrotron x-ray phase-contrast imaging study of the primary breakup mechanism of a coaxial air-assisted water jet. There exist great similarities between the primary (jet) and the secondary (drop) breakup, and in the primary breakup on different length scales. A transition from a ligament- to a membrane-mediated breakup is identified around an effective Weber number $We' \sim 13$. This observation reveals the critical role an effective Weber number plays in determining the atomization process and strongly supports the cascade breakup model.

DOI: 10.1103/PhysRevLett.100.154502 PACS numbers: 47.20.Ft, 47.20.Lz, 47.20.Ma

Liquid jet atomization into droplets has wide scientific and technological applications. The recent resurgent interest in low-speed liquid jet breakup lies in the finite-time singularities associated with them and have shown some complex self-similar behavior at different length scales [1,2]. The physics of high-speed liquid jet atomization is less clear and still not well understood [3,4] due to its complexity and transient nature. It is generally believed that the atomization process consists of removing liquid mass from the surface to form big liquid drops and breaking up these big drops subsequently into smaller ones. These two distinctive subprocesses are conventionally termed primary and secondary breakup.

The study of the atomization process traditionally follows cascade models [5] based on the turbulence model of Kolmogorov [6]. However, these oversimplified theoretical models do not match the complex breakup phenomena observed in the experiments and this fact prompted system-specific [7,8] or empirical models [4] to describe the breakup process. Recently, a ligament-mediated breakup model was proposed [7,8] to describe the primary breakup of a coaxial air-assisted water jet which is not based on the cascade idea [9]. However, there also exists certain support of the cascade model. Varga *et al.* [10] studied a small-diameter liquid jet exposed to a very high-speed airstream and observed that there exist some similarities between the liquid jet and droplet breakup qualitatively [4,10]. In this Letter, we report a detailed study of the primary breakup process of a coaxial air-assisted water jet over a wide air speed range by ultrafast synchrotron x-ray phase-contrast imaging technique. By exploiting the unprecedented spatial and temporal resolutions offered by this new technique, we have established the close analogy between the breakup phenomenology at different length scales (jet-primary or undulation-primary) and for different initial conditions (jet breakup or drop breakup) quantitatively. Our experiment provides strong support for the cascade model. The ligament-mediated breakup model [7,8] remains a relatively low air speed approximation.

A commercial paint spray gun is employed to generate the coaxial air-assisted water spray. The spray gun has a central circular orifice with diameter of 1.1 mm. The coaxial air annular orifice has an inner diameter of 2.48 mm and outer diameter of 3.90 mm. The water emanates from the central orifice with considerably lower speed as compared to the coflowing air. The breakup phenomenon is studied in a wide air speed range with fixed water flow speed. The cross-section averaged water and air speeds at the nozzle exit are measured by the water flow rate and by a commercial air velocity analyzer (SEAVA®). With water flows at 8.3 m/s, the liquid Reynolds number ($\mathrm{Re} = V_l D_l/\upsilon_l$) is 6000, where V_l denotes the water exit velocity, D_l the water jet diameter, and υ_l the water dynamic viscosity. However, since the nozzle tip has a high contraction ratio (~ 7.2), the turbulence is not fully developed for both the water and airstream. The jet Weber number [$\mathrm{We} = \rho_g(V_g - V_l)^2 D_l/\sigma$] can also be defined, in which ρ_g denotes the air density, V_g the air exit velocity, and σ the water surface tension.

The primary breakup process is studied by ultrafast x-ray phase-contrast imaging technique on 32-ID beam line at the Advanced Photon Source (APS) of Argonne National Laboratory. The "white beam" (unfiltered full energy spectrum) x-ray radiation from the undulator delivers the necessary x-ray flux for the temporal and spatial resolutions required for this experiment. The undulator gap was set to 31 mm to give a 13.3 keV first harmonic in the x-ray energy spectrum. The image contrast is dominated by phase contrast instead of absorption contrast [11–13]. The transmitted and diffracted x rays through the jet are converted to visible lights by a scintillator crystal (LYSO:Ce) placed at 750 mm downstream from the sample and imaged with optical lenses ($5\times$, NA = 0.14) onto a fast CCD camera (SensiCam SVGA from Cooke Corp., 1024×1280 pixels chip). The effective size of each pixel after optical magnification is $1.25 \times 1.25\ \mu\mathrm{m}^2$. The effective imaging resolution and field of view are 2.4 μm and $1.37 \times 1.71\ \mathrm{mm}^2$, respectively.

 © 2008 The American Physical Society

The breakup process was studied by a combination of single-exposure and multiple-exposure imaging schemes. In the single-exposure scheme, the snapshots of the breakup process were taken with a single 472 ns x-ray pulse. The multiple-exposure scheme takes advantage of the repetitive temporal structure of the x-ray pulses generated from the synchrotron storage ring (a 472 ns x-ray pulse is generated every 3.68 μs) to catch the breakup dynamics. An 18.4 μs exposure interval was adopted to match the speed of the dynamics of interest. Exploiting this scheme, we can catch the breakup dynamics in a single image frame.

In Fig. 1, the single-exposure images of the water jet with different air speeds are shown. The image frames taken at different distances from the nozzle exit were stitched together to give an overall view of the breakup process (frames were not taken concurrently). Since our field of view is just slightly bigger than the jet diameter, only the upper half of the jet was imaged.

Qualitative differences of the breakup at different air speeds are easily recognizable. The airstream induces surface undulations in all occasions. These surface undulations occur more chaotically as compared to previous studies [7,8]. They develop earlier and with bigger amplitudes as the air speeds increase and eventually cause the water mass disintegration from the main jet. We observed that only when the air speed is higher than 42 m/s that these surface undulations are responsible for the breakup of the liquid mass from the main jet. Below that speed, water jet breaks up as a whole through Rayleigh-Plateau instability. The study of the exact velocity boundary between these two regimes is beyond the scope of the current work due to our limited field of view.

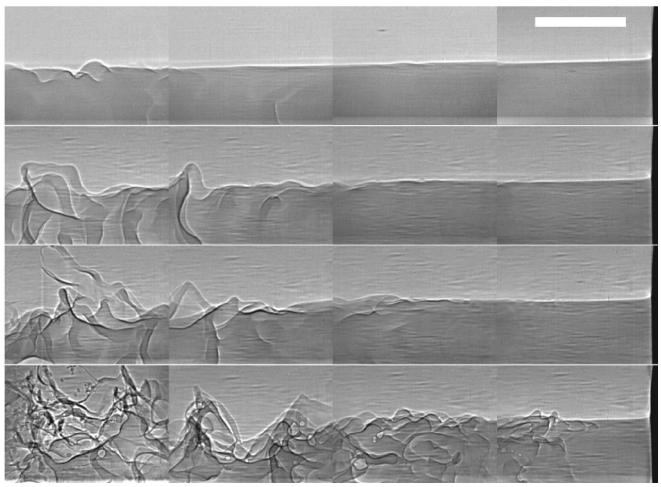

FIG. 1. X-ray 472 ns single-exposure phase-contrast images of the water jet with increasing air velocities. The jets are injected from the right sides of the figures. The nozzle exit air speeds are 32.5 m/s, 61.6 m/s, 71.0 m/s, and 102 m/s from top to bottom. The scale bar denotes 1 mm.

To understand the undulation-induced breakup process more closely, we carefully focus on the surface undulations by taking their snapshots and following their dynamics. Experimentally, we noticed that the breakup process falls into two distinctive scenarios when $V_g < 60$ m/s or $V_g > 60$ m/s.

When $V_g < 60$ m/s, the surface undulations are amplified as they move downstream and form rodlike structures protruding into the air [Fig. 2(a)]. The breakup happens in which a big lump of liquid mass disintegrates from the jet, as shown in Fig. 2(b) when $V_g = 50.9$ m/s. The retracting neck and capillary waves excited at both ends can be clearly seen. Satellite droplets are much smaller than the main droplet.

When the air speeds are further increased, the surface rods are stretched more to form long ligaments and break up subsequently, as is clear from Figs. 3(a) and 3(b) when $V_g = 57.6$ m/s. The ligament breaks off through an ''end pinching'' mechanism as suggested by Stone [14]. The ''end pinching'' happens at the neck of the end blob and the pinching time is determined by the capillary time $t_c = (\frac{\rho_l r^3}{\sigma})^{1/2}$ [3], where ρ_l is the liquid density, and r is the blob radius. As shown in Fig. 3(a), the breakup is almost complete after only three consecutive exposures, in agreement with the capillary time (~ 55 μs) determined by the end blob radius (~ 80 μm). Once the pinchoff of the blob from the ligament is complete and the aerodynamic stretching forces on the ligament disappear, the remaining ligament will retract and break up due to capillary insta-

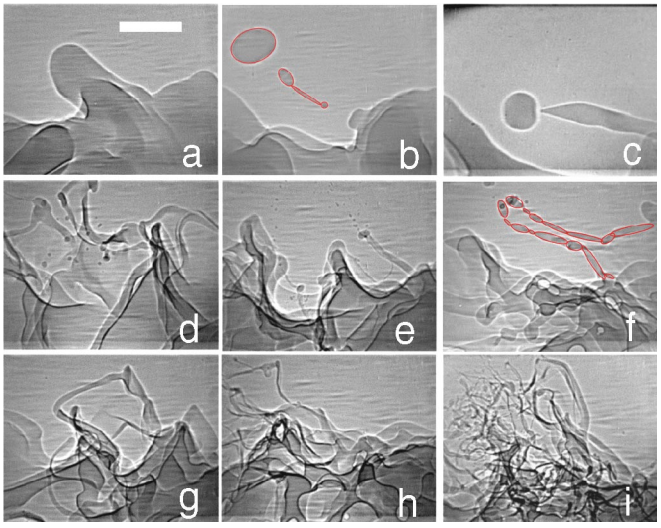

FIG. 2 (color). Characteristic single-exposure surface undulation-induced breakup images for increasing air speeds. (a),(b) $V_g = 50.9$ m/s; (c) $V_g = 52.9$ m/s; (d)–(f) $V_g = 71.0$ m/s; (g) $V_g = 87.1$ m/s; (h), (i) $V_g = 102$ m/s. The red lines indicate the procedures adopted to estimate the breakup volume V_{break} for both ligament- and membrane-mediated breakups. The scale bar denotes 0.5 mm.

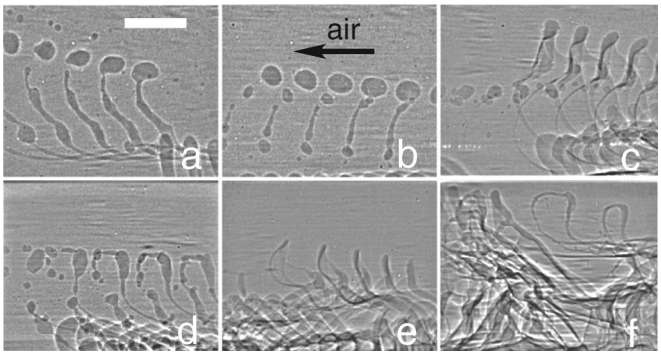

FIG. 3. Multiple-exposure images of the breakup dynamics. (a),(b) $V_g = 57.6$ m/s; (c),(d) $V_g = 61.6$ m/s; (e) $V_g = 71.0$ m/s; (f) $V_g = 87.1$ m/s. Exposures are earlier in time at the right sides, the interval between exposures is 18.4 μs. The scale bar denotes 0.5 mm.

bilities. Interestingly, the lump liquid mass breakup to ligament breakup transition resembles greatly the dripping to jetting transition in low-speed jet breakup [15].

The breakup changes drastically when the air speed is above 60 m/s. Instead of forming ligaments, the preformed surface undulations were blown into two-dimensional membrane structures with thick rims. The membrane structures continue to expand in the wind and eventually burst. As a result, the rim collects most of the liquid mass and breaks up in a secondary step due to capillary instabilities. Figures 2(d)–2(f) plot the snapshots of different stages of the membrane-mediated breakup when V_g is 71.0 m/s, and Figs. 3(c) and 3(d) illustrate in detail the breakup process through the multiple-exposure imaging technique. In Fig. 3(d), it is observed that after the bursting of the membrane, the remaining rim is further stretched in the airstream. It breaks up in very similar fashion as the ligaments due to capillary instabilities.

Very high air speed cases are more difficult to study since the breakup happens more chaotically. As shown in Figs. 2(g)–2(i), when the air speed is above 87 m/s, the breakup process is characterized by a large number of fine threads. However, the membranes can still be seen with much thinner rims, with the dynamics captured in Fig. 3(f). It is natural to presume that the generation of fine threads is still owing to the breakup of thinner membranes.

In sum, the undulation-induced breakup process displays a family of rich phenomena as possessing both ligament- and membrane-mediated breakups. It has to be emphasized that these types of breakups are different from previous studies [4] in which the jet as a whole breaks up through the Rayleigh and membrane breakup. In our case, the breakup happens by peeling off liquid mass through the surface undulations while the main jet remains relatively steady. Our corresponding jet Weber number is more closely related to the "fiber breakup" regime in previous studies [4].

The surface undulation-induced ligament- and membrane-mediated breakups observed in the current study resemble greatly the droplet breakups in a high-speed airstream. The similarity does not seem to be coincidental. When a droplet breaks up in high-speed airstream, there exists reflection symmetry of the breakup against the meridional plane [9]. As shown in Fig. 4, the surface undulations are exposed to the high-speed airflow once formed. Since the dimension of the surface undulation is normally much smaller than the jet diameter, its dynamics can be treated quite independently from that of the main jet. As a result, the surface undulation in high-speed airflow could be treated as a half liquid sphere by approximation [9]. Our experiment revealed that this phenomenological conjecture seems surprisingly self-consistent. To establish this analogy quantitatively, we calculated the effective Weber number $[\mathrm{We}' = \rho_g(V_g - V_l)^2 D_{\mathrm{undulation}}/\sigma]$ of the surface undulations by its effective diameter (estimated by summing up the breakaway volume V_{break} in a single breakup event), where $D_{\mathrm{undulation}}$ is the equivalent half sphere diameter which has the same volume with V_{break} [$V_{\mathrm{break}} = 2\pi/3(D_{\mathrm{undulation}}/2)^3$].

Since the imaging process is by nature two-dimensional, careful precautions were taken in estimating V_{break}. In the ligament-mediated breakup case, the volume integration is either estimated by adding up all individual droplet volumes assuming that fairly spherical droplets are formed, or assuming an axial symmetry along the ligament axis, and dividing the ligaments into small regions for integration as illustrated in Figs. 2(b) and 2(f). In the membrane-mediated breakup regime, the integration is trickier since the membrane itself can carry substantial mass and there is no obvious symmetry in the system. As a result, the integration is carried out after the membrane bursts, the re-

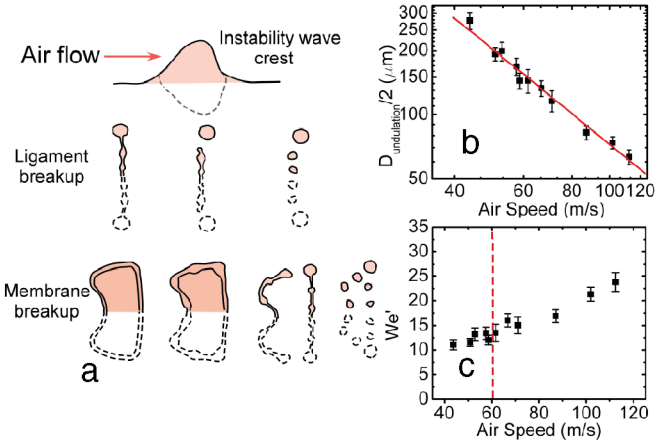

FIG. 4 (color). Panel (a) shows the schematic of a surface undulation in comparison with a half droplet. The ligament- and membrane-mediated breakup modes observed in the experiment are illustrated schematically. Panel (b) shows the effective $D_{\mathrm{undulation}}$ as a function of air speeds. Panel (c) shows the corresponding We′ as a function of air speed. The transition from ligament- to membrane-mediated breakup happens around $\mathrm{We}' \sim 13$ ($V_g \sim 60.0$ m/s).

maining frame has local axial symmetry, and the retracting membrane carries negligible mass except at its boundary rims. In total, about 200 events were integrated for both ligament- and membrane-mediated breakups.

Two results stand out instantly once the effective breakup radii for different air speeds are obtained. A log scale plot shows a clear power law relationship between the air speed and the effective breakup radius $D_{\text{undulation}} \sim V_g^{-3/2}$. Our data follow the same trend as a similar figure by Marmottant *et al.* [7] and extend it to a higher velocity range to include the transition from the ligament- to membrane-mediated breakup. This agreement is very surprising given the highly chaotic nature of our breakup process. On the other hand, it implies that the breakup is mostly determined by fundamental parameters such as Weber number since the breakup is controlled by the competition between the aerodynamic force and the liquid surface tension.

It is observed that the undulations break up under ligament-mediated breakup mode for $\text{We}' < 13$, and a membrane-mediated breakup mode for $\text{We}' > 13$. This is in excellent agreement with the Weber number ranges observed for droplet breakup transition from stretching to membrane breakup in high-speed airstream [16,17]. Thus, this observation suggests that the two phenomena have intrinsic connections owing to the quantitative match in both the Weber number and the breakup phenomenology.

The presumption that the undulation dynamics can be treated fairly independently from the main jet dynamics can also be justified by the fact that, when the air speed is fairly high, each breakup event will remove liquid mass with much smaller radii than the water jet diameter (Fig. 4). Only when the air speed approaches zero, the effective breakup diameter will diverge so that the dynamics of the jet has to be included, in which we encounter the familiar jet Rayleigh and membrane breakup [4]. Not surprisingly, a transition between these two breakup modes happens at a similar Weber number as in our undulation case when the jet Weber number is used.

This additional analogy between the jet-primary and the undulation-primary breakups [4,18] adds further support for the cascade breakup model [5]: the great similarities of the primary breakups at different length scales suggest that an effective Weber number on different length scales can be defined and the breakup is mainly dependent upon it. The complex high-speed liquid breakup will display self-similar behavior as its low-speed counterpart on different length scales repeatedly. As a result, when energy dissipation at different length scales is known such as in a turbulence breakup scenario [5], the breakup process can be determined by recursively applying the low-speed breakup results for different length scales. It is interesting to see if the eventual log-normal droplet size distribution is reached when more stages of the cascade process are added.

It is well known that one of the dominant difficulties of the jet-breakup research has been the complexity of the processes involved; direct simulation is practically impossible [17,19]. In the current Letter, we have made progress in establishing the self-similar breakup phenomenology displayed in high-speed liquid jet breakup and we believe it will lead to great insights into this field of research.

The authors thank Paul Micheli and Jin Wang for providing the spray gun system. This work and the use of the APS are supported by the U.S. Department of Energy, Office of Science, Office of Basic Energy Sciences, under Contract No. DE-AC02-06CH11357, and Argonne National Laboratory Director's Competitive Grant (LDRD) No. 2006-023-N0.

[1] J. Eggers, Rev. Mod. Phys. **69**, 865 (1997).
[2] J. X. D. Shi, M. P. Brenner, and S. R. Nagel, Science **265**, 219 (1994).
[3] Y. J. Wang *et al.*, Appl. Phys. Lett. **89**, 151913 (2006).
[4] N. Chigier and R. D. Reitz, in *Recent Advances in Spray Combustion: Spray Atomization and Drop Burning Phenomena*, edited by K. K. Kuo (AIAA, New York, 1996), Vol. 1, pp. 109–135.
[5] E. A. Novikov and D. G. Dommermuth, Phys. Rev. E **56**, 5479 (1997).
[6] A. N. Kolmogorov, Dokl. Akad. Nauk SSSR **66**, 825 (1949).
[7] P. Marmottant and E. Villermaux, J. Fluid Mech. **498**, 73 (2004).
[8] E. Villermaux, P. Marmottant, and J. Duplat, Phys. Rev. Lett. **92**, 074501 (2004).
[9] Y. Pomeau and E. Villermaux, Phys. Today **59**, No. 3, 39 (2006).
[10] C. M. Varga, J. C. Lasheras, and E. J. Hopfinger, J. Fluid Mech. **497**, 405 (2003).
[11] A. Snigirev *et al.*, Rev. Sci. Instrum. **66**, 5486 (1995).
[12] T. J. Davis *et al.*, Nature (London) **373**, 595 (1995).
[13] S. W. Wilkins *et al.*, Nature (London) **384**, 335 (1996).
[14] H. A. Stone, Annu. Rev. Fluid Mech. **26**, 65 (1994).
[15] B. Ambravaneswaran, H. J. Subramani, S. D. Philips, and O. A. Basaran, Phys. Rev. Lett. **93**, 034501 (2004).
[16] M. Pilch and C. A. Erdman, Int. J. Multiphase Flow **13**, 741 (1987).
[17] Z. Liu and R. D. Reitz, Int. J. Multiphase Flow **23**, 631 (1997).
[18] J. C. Lasheras and E. J. Hopfinger, Annu. Rev. Fluid Mech. **32**, 275 (2000).
[19] S. Zaleski, J. Li, and S. Succi, Phys. Rev. Lett. **75**, 244 (1995).